Tumor promotion by caspase-resistant retinoblastoma protein

Helena L. Borges*†‡, Jeff Bird*†, Katherine Wasson§, Robert D. Cardiff§, Nissi Varki*¶, Lars Eckmann†, and Jean Y. J. Wang*†‖

*Division of Hematology/Oncology, Moores Cancer Center, and Departments of †Medicine and ¶Pathology, School of Medicine, University of California at San Diego, La Jolla, CA 92093; and §Center for Comparative Medicine, University of California, Davis, CA 95616

Edited by Xiaodong Wang, University of Texas Southwestern Medical Center, Dallas, TX, and approved September 9, 2005 (received for review May 11, 2005)

The retinoblastoma (RB) protein regulates cell proliferation and cell death. RB is cleaved by caspase during apoptosis. A mutation of the caspase-cleavage site in the RB C terminus has been made in the mouse *Rb-1* locus; the resulting *Rb-MI* mice are resistant to endotoxin-induced apoptosis in the intestine. The *Rb-MI* mice do not exhibit increased tumor incidence, because the *MI* mutation does not disrupt the *Rb* tumor suppressor function. In this study, we show that *Rb-MI* can promote the formation of colonic adenomas in the *p53-null* genetic background. Consistent with this tumor phenotype, *Rb-MI* reduces colorectal epithelial apoptosis and ulceration caused by dextran sulfate sodium. By contrast, *Rb-MI* does not affect the lymphoma phenotype of *p53-null* mice, in keeping with its inability to protect thymocytes and splenocytes from apoptosis. The Rb-MI protein is expressed and phosphorylated in the tumors, thereby inactivating its growth suppression function. These results suggest that RB tumor suppressor function, i.e., inhibition of proliferation, is inactivated by phosphorylation, whereas RB tumor promoting function, i.e., inhibition of apoptosis, is inactivated by caspase cleavage.

apoptosis | dextran sulfate sodium | p53-knockout | tumor promoter | tumor suppressor

Carcinogenesis is a multistep process involving epigenetic and genetic factors. The role of genetic alterations in tumor development is well established through the identification of proto-oncogenes and tumor suppressor genes, which control cell proliferation, differentiation, and death (1). The coordinated actions of these proteins maintain tissue homeostasis, the irreversible disruption of which underlies tumor formation. The tumor suppressors RB and p53 are important regulators of the cell cycle and apoptosis; their functions are disrupted in a large fraction of sporadic human cancers (1). The disruption of p53 is mostly through mutation of the *p53* gene, whereas the disruption of RB is generally mediated by its hyperphosphorylation (2). Consistent with its tumor suppression function, the nuclear RB protein inhibits cell cycle progression and promotes terminal differentiation (3–5). Inconsistent with tumor suppression, however, RB also inhibits apoptosis (3). The biallelic inactivation of *RB* gene, either in human cancers or in *Rb*-knockout mice, sensitizes cells to mitogenic and apoptotic stimuli (3).

RB regulates E2F, a family of transcription factors that control the expression of genes required for DNA replication and for apoptosis (6–9). Loss of RB leads to the activation of E2F and, thus, resulting in enhanced response to mitogenic and apoptotic factors. RB also regulates the nuclear Abl tyrosine kinase, which stimulates apoptosis when activated by genotoxins or tumor necrosis factor (TNF) (10–12). The proapoptotic function of E2F-1, the major partner of RB among the E2F family, has been linked to the transcriptional up-regulation of p19Arf and p73 (13–17). The increased expression of p19Arf leads to the stabilization of p53 through the disruption of Mdm2–p53 interaction (18, 19). Genetic ablation of both p53 and p73 is required to block E2F-1 from causing apoptosis in mouse fibroblasts (7, 13). Interestingly, nuclear Abl kinase also activates p53 and p73, enhancing the stability and function of these two proteins (10, 11). Genetic ablation of p73 is sufficient to block cell death induced by a constitutively activated nuclear Abl in mouse fibroblasts (20). Because the inactivation of RB causes cells to be permissive for proliferation and vulnerable to apoptosis, loss of RB must be combined with apoptosis resistance to promote tumor development (3). Mutation of the *p53* gene can compromise the proapoptotic function of E2F and Abl, thereby allowing the loss of RB to drive uncontrolled proliferation. Thus, the combined ablation of the *Rb* and *p53* genes increases tumor incidence in mouse models (18, 19), and the disruption of both RB and p53 is prevalent in sporadic human cancers.

The RB protein is a substrate of cyclin-dependent protein kinases during cell cycle progression (21–23). Phosphorylation site-mutated RB blocks cell-cycle progression, demonstrating phosphorylation to inactivate the RB growth suppression function (24). The RB protein is also a substrate of caspase, and it is cleaved during apoptosis (25). We have previously mutated the major caspase cleavage site, $_{884}$DEADG$_{888,}$ at the RB C terminus and have shown the resulting RB-MI protein to be resistant to cleavage and subsequent degradation in apoptotic cells (26). Ectopic expression of RB-MI protects mouse fibroblasts from TNF-induced death and granular neurons from depolarization-induced apoptosis (26, 27). This C-terminal caspase cleavage site has also been eliminated by knock-in mutation in the mouse germ line to generate the *Rb-MI* allele (28). The *Rb-MI* allele afforded protection from endotoxic shock in male mice (28). Apoptosis associated with endotoxic shock is attenuated in the intestine, but not in the spleen, of *Rb-MI* mice (28). Fibroblasts derived from *Rb-MI* embryos are resistant to apoptosis induced by the type I receptor for tumor necrosis factor (TNFRI) (28). These results suggest RB cleavage by caspase is required for TNFRI-induced cell death. The *Rb-MI* mice are healthy, fertile, and do not exhibit increased tumor incidence. Thus, the tumor suppression function of *Rb* is not disrupted by the *MI* mutation. However, the antiapoptotic function of *Rb-MI* raises the interesting possibility that it might promote tumor formation, particularly under conditions when its tumor suppression function can be inactivated. To test this hypothesis, we combined the *Rb-MI* allele with the ablation of the mouse *p53* gene. Our study has revealed *Rb-MI* to promote colon tumor in *p53-null* background. As would be predicted, Rb-MI protein is expressed and phosphorylated in these *p53-null* tumors. Our results suggest that cleavage of RB by caspase is a critical step in apoptotic response

This paper was submitted directly (Track II) to the PNAS office.

Freely available online through the PNAS open access option.

Abbreviations: DSS, dextran sulfate sodium; RB, retinoblastoma.

‡Present address: Instituto de Ciencias Biomedicas, Departamento de Anatomia, Universidade Federal do Rio de Janeiro, Centro de Ciencias da Saude, 21.940-900, Rio de Janeiro, Brazil.

‖To whom correspondence should be addressed. E-mail: jywang@ucsd.edu.

to inflammation and injury in the intestine and that disruption of this event can promote tumor formation.

Materials and Methods

Mice. The $p53^{+/-}$ mice (*Trp53tm*) were purchased from The Jackson Laboratory. Construction of the mouse *Rb-MI* allele was described in ref. 28. The $p53^{+/-}$ and the $Rb^{+/MI}$ mice were backcrossed for 6–7 generations into the 129S6/SvEvTac background. Genotyping was performed as described in refs. 28 and 29. Moribund mice were killed by CO_2 asphyxiation, their tissues were collected, fixed with 10% phosphate buffered formalin, embedded in paraffin, sectioned, and stained.

Dextran sulfate sodium (DSS) salt (3%, 36,000–50,000 Da, ICN Biomedical) was added to the drinking water of male adult mice for either 3 or 7 days. Animals were monitored daily for fecal blood and body weight. The water consumption was monitored and found to be similar among mice of different genotypes. Animals were killed on day 3 or day 8 (one day on regular drinking water after 7 days on DSS water), and their colons were removed and processed for histology. All animal studies were approved by the University of California at San Diego institutional animal care and use committee.

Statistical analysis was performed by using PRISM 4 (2003) from GraphPad (San Diego). The histograms display the mean and standard error (s.e.m.).

Immunohistochemistry. Deparaffinized, rehydrated, and unstained sections were boiled in 10 mM sodium citrate buffer (pH 6.0) for 12 min to retrieve antigen. Immunostaining was carried out with anti-RB-851 (30), mouse anti-RB (G3–245, BD Biosciences), anti-proliferating cell nuclear antigen (Calbiochem), anti-Ki-67 (Ab 833-500, Abcam, Inc.) and anti-β catenin (Ab 15180, Abcam, Inc.) with standard immunohistochemistry protocols. For detection of phosphorylated RB, rabbit anti-RB-phospho-Ser-807/811 (Cell Signaling Technology) and goat anti-RB-phospho-Thr-821/826 (Santa Cruz Biotechnology) were used, and the detection was by fluorescent immunohistochemistry with the TSA kit (Promega). After antigen retrieval, slides were further incubated with a phosphatase inhibitor (100 nM Calyculin A, Calbiochem) for 20 min at 37°C in Tris-buffered saline (20 mM Tris, pH 7.5/150 mM NaCl). Tissues were blocked with 5% normal donkey serum in TBS with 0.2% Triton X-100 (blocking solution). Phospho-RB antibody was diluted 1:100 in blocking solution and incubated for 16 h at 4°C. Horseradish peroxidase (HRP)-conjugated secondary antibody was then added onto the tissue section after an extensive wash. The HRP activity catalyzes the deposit of Alexa Fluor 488 tyramide at the site of staining to amplify signals for easy detection. To prepare the tissue section for staining with the second antibody, the HRP activity from the previous round of staining was inactivated by treatment with hydrogen peroxide. The sections were then incubated with threonine-specific phospho-RB antibody (1:200) and subjected to a similar signal amplification procedure, except that Alexa Fluor 555 tyramide was used as the fluorochrome (Promega). Finally, the tissue sections were counterstained with 10 μg/ml Hoechst 33258 dye (Sigma) and incubated with cupric solution (10 mM $CuSO_4$/50 mM ammonium acetate, pH 5.0) to decrease auto fluorescence.

To control for the specificity of phosphoantibodies, tissue samples were dephosphorylated with 10 units/μl calf intestinal alkaline phosphatase (New England Biolabs). After washing, immunohistochemistry was performed as described above. Further immunohistochemistry controls were performed by omitting the primary antibody from the reactions. Additional negative control was performed by using the isotype control for the anti-RB antibody (BD Biosciences).

Terminal deoxynucleotidyl transferase-mediated dUTP nick-end labeling assay (TUNEL) was performed according to the manufacturer's protocol (Roche Diagnostic). TUNEL-positive nuclei were counted in 30 fields starting with the most distal colorectal epithelium under the microscope at $\times$400 magnification.

Microbial Analysis. Fecal samples were analyzed for *Helicobacter* by using polymerase chain reactions performed by the Research Animal Diagnostic laboratory at the University of Missouri, Columbia. Hematoxylin/eosin-stained colonic tissue slices were examined for bacteria and protozoa by morphology and for *Helicobacter* by polymerase chain reactions by standard methods, with murine GAPDH as a control, which was detected in each sample.

Results

***Rb-MI* Does Not Affect the Incidence of Lymphomas.** The *Rb-MI* allele is transmitted according to the Mendelian ratio (28). We have maintained the *Rb-MI* breeding colonies for several years and did not observe shortened lifespan with either $Rb^{+/MI}$ or $Rb^{MI/MI}$ mice. Thus, *Rb-MI* does not predispose mice to the initiation of spontaneous tumors. To test whether *Rb-MI* has tumor promotion function, we introduced it into the *p53-null* genetic background. Double heterozygous mice, $Tm(Rb^{MI/+}xp53^{+/-})$, were intercrossed to generate the experimental cohort. The $Tm(Rb^{+/+}xp53^{-/-})$ and $Tm(Rb^{MI/MI}xp53^{-/-})$ mice were born according to the Mendelian ratio. In the $p53^{+/+}$ background, mice with either $Rb^{+/+}$ or $Rb^{MI/MI}$ genotype did not develop lymphomas during the time period when the majority of mice in the $p53^{-/-}$ background became moribund with disseminated lymphoma involving various tissues (Fig. 4*A*, which is published as supporting information on the PNAS web site). We found that the *Rb-MI* allele did not alter the frequency of lymphoma or the course of this disease in the $p53^{-/-}$ mice (Table

Table 1. Tumor spectrum and incidence of the major tumor types

Genotype	Lymphoma,* %	Teratoma,* %	Colon neoplasm,† %	Others,‡ %	No. of mice
$Tm(Rb^{+/+}\ xp53^{-/-})$	75	18	3	8	40
$Tm(Rb^{+/MI}\ xp53^{-/-})$	63	32	15§	13	53
$Tm(Rb^{MI/MI}\ xp53^{-/-})$	67	28	26¶	13	54

*No statistical difference in the incidence of lymphoma or teratoma among the three genotypes.

†Percent of moribund animals with colon tumors (adenoma or adenocarcinoma), excluding animals that died with teratoma.

‡Percent of moribund animals with soft tissue sarcomas (hemangiosarcomas, osteosarcomas, or rhabdomyosarcomas) or lung adenoma.

§Statistical analysis of tumor incidence in $Tm(Rb^{+/+}\ xp53^{-/-})$ and $Tm(Rb^{MI/MI}\ xp53^{-/-})$ mice showed $P > 0.05$ (Fisher's exact test).

¶Statistical analysis of tumor incidence in $Tm(Rb^{+/+}\ xp53^{-/-})$ and $Tm(Rb^{MI/MI}\ xp53^{-/-})$ showed $P = 0.0196$ (Fisher's exact test).

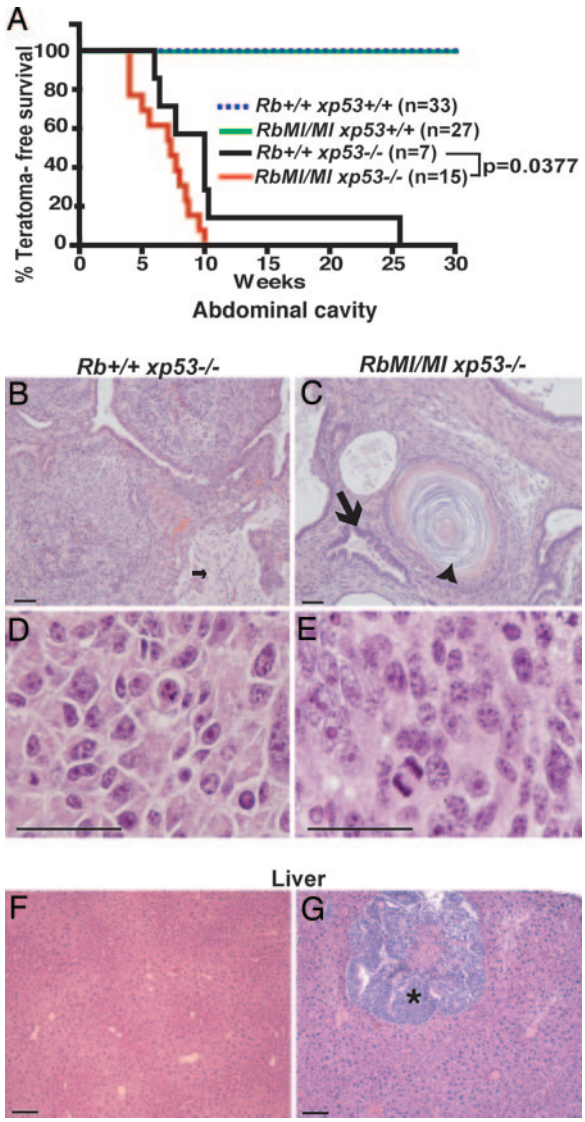

Fig. 1. Teratomas in $Tm(Rb^{MI/MI}xp53^{-/-})$ mice. (*A*) Kaplan-Meier survival curve of animals that died with teratoma ($P = 0.0377$, Log-rank test comparing $Rb^{+/+}xp53^{-/-}$ with $Rb^{MI/MI}xp53^{-/-}$). (*B* and *C*) Representative photomicrographs of hematoxylin/eosin-stained paraffin sections of differentiated tumor areas. (*D* and *E*) Representative photomicrographs of hematoxylin/eosin-stained paraffin sections of less differentiated, highly cellular tumor areas. (*F* and *G*) Photomicrographs of normal liver (*F*) and germ cell tumor expanding into the liver (*G*, asterisk) in mice with the indicated genotypes. Small arrow in *B* shows brain-like tissue. Large arrow in *C* indicates epithelium, and arrowhead indicates laminar keratin structure. (Scale bars: 100 μm.)

1 and Fig. 4 *B–E*). The mean survival time of $p53^{-/-}$ mice with aggressive lymphoma was 18 weeks, irrespective of the *Rb*-genotype (+/+ or *MI*/*MI*) (Fig. 4*A*). The frequency of infiltration to other organ sites, including liver, lung, kidney, or heart, was statistically similar between $Tm(Rb^{+/+}xp53^{-/-})$ and $Tm(Rb^{MI/MI}xp53^{-/-})$ mice (Table 1 and Fig. 4 *B–E*).

Effect of *Rb-MI* on Teratomas. Owing to the 129/Sv background, teratoma was the second most frequent tumor type in the $p53^{-/-}$ mice (31). Mice in the $p53^{+/+}$ genetic background, irrespective of their *Rb* genotypes, did not develop teratomas (Fig. 1*A*). The incidence of testicular tumors in $Tm(Rb^{MI/MI}xp53^{-/-})$ mice was higher than in $Tm(Rb^{+/+}xp53^{-/-})$ mice (Table 1). The median survival of mice with teratomas was 7 weeks for $Tm(Rb^{MI/MI}xp53^{-/-})$ and 10 weeks for $Tm(Rb^{+/+}xp53^{-/-})$ mice (Fig. 1*A*). The teratomas often expanded to the abdominal cavity and showed cystic elements that were histologically characterized as keratinizing epithelium, glandular epithelium, cartilage, and bone and neuronal tissues (Fig. 1 *B* and *C*). Less differentiated areas, characterized by increased cellularity and mitotic rates, were also found in these tumors in both $Tm(Rb^{+/+}xp53^{-/-})$ and $Tm(Rb^{MI/MI}xp53^{-/-})$ mice (Fig. 1 *D* and *E*). We found that a higher percentage of teratomas from $Tm(Rb^{MI/MI}xp53^{-/-})$ mice had necrosis with hemorrhage, likely due to a higher rate of tumor expansion, and were more frequently associated with metastasis (Fig. 1*G*). Approximately 30% of $Tm(Rb^{MI/MI}xp53^{-/-})$ mice that lived beyond the median survival time showed extratesticular teratomas in lung, liver, lymph nodes, and/or pancreas, whereas no extratesticular teratomas were evident in $Tm(Rb^{+/+}xp53^{-/-})$ mice (Fig. 1 *D* and E). These results suggested that *Rb-MI* exacerbated the phenotype of teratomas in the *p53-null* genetic background.

***Rb-MI* Increases the Incidence of Colon Tumors.** In moribund mice with disseminated lymphoma, necropsy revealed an *Rb-MI*-dependent increase in the incidence of colon tumors (Table 1 and Fig. 2). The majority of colon tumors in $Tm(Rb^{MI/MI}xp53^{-/-})$ mice displayed characteristics of a sessile type of adenoma (Fig. 2*C*). The adenomas were comprised of irregular glands with an abundance of mitotic figures and a reduction in the number of goblet cells. Thus, *Rb-MI* increased the incidence of colon adenomas in mice that also developed lymphoma (Fig. 2*G*). We also observed aggressive adenocarcinoma of the colon (Fig. 2 *E* and *F*), characterized by an invasive tumor mass with irregular, densely crowded proliferating glands comprised of cells with large pleomorphic, hyperchromatic nuclei, prominent nucleoli, and abnormal mitoses. The tumor extended through the muscularis mucosa, the submucosa, and the muscularis, reaching the pericolonic fat (Fig. 2*E*). Among 31 $Tm(Rb^{+/+}xp53^{-/-})$ mice with lymphoma, only one developed adenocarcinoma in the colon (Fig. 2*G*), consistent with previously published reports that a colonic tumor is a rare phenotype of *p53-null* mice (29, 31). However, introduction of the *Rb-MI* allele significantly increased the incidence of colonic tumors, particularly adenomas (Table 1 and Fig. 2*G*).

The colon tumors in $Tm(Rb^{MI/MI}xp53^{-/-})$ mice were frequently found to have a mixture of inflammatory infiltrates with macrophages, eosinophils, neutrophils, and lymphocytes within the tumor areas (Fig. 2*C*). The luminal surface of the tumor tissues were composed of epithelial cells with poor polarization and alignment, indicating disruption of the epithelial barrier. In two colon tumors, epithelial dysplasia associated with tissue repair was observed, suggesting that the tumor-adjacent normal epithelium was affected by the tumor-associated ulcerations and mucosal inflammation. Inflammatory infiltrates were not detected in tumor-free tissues from *p53-null* mice of $Rb^{+/+}$, $Rb^{+/MI}$, or $Rb^{MI/MI}$ genotype (data not shown). This observation suggests that *Rb-MI* did not render mice more prone to spontaneous or infection-related colonic inflammation, a potential contributor to colon tumor development (32). We also examined the incidence of infection with *Helicobacter* spp., a group of bacteria that has been implicated in murine colon tumorigenesis (33), in fecal samples or tumor sections and found the incidence to be similar among the different mouse strains in the experimental cohort (data not shown). These results do not rule out the involvement of infection and inflammation in colonic tumor development but suggest that *Rb-MI* is not likely to promote tumor formation by predisposing mice to infection or inflammation.

For *Rb-MI* to promote tumor development, the Rb-MI protein should be expressed and its growth suppression function inactivated in tumor cells. In a majority of sporadic human cancers, RB is inactivated by phosphorylation (1, 2). We used two antibodies, reacting with phosphorylated Ser-807/811 or phos-

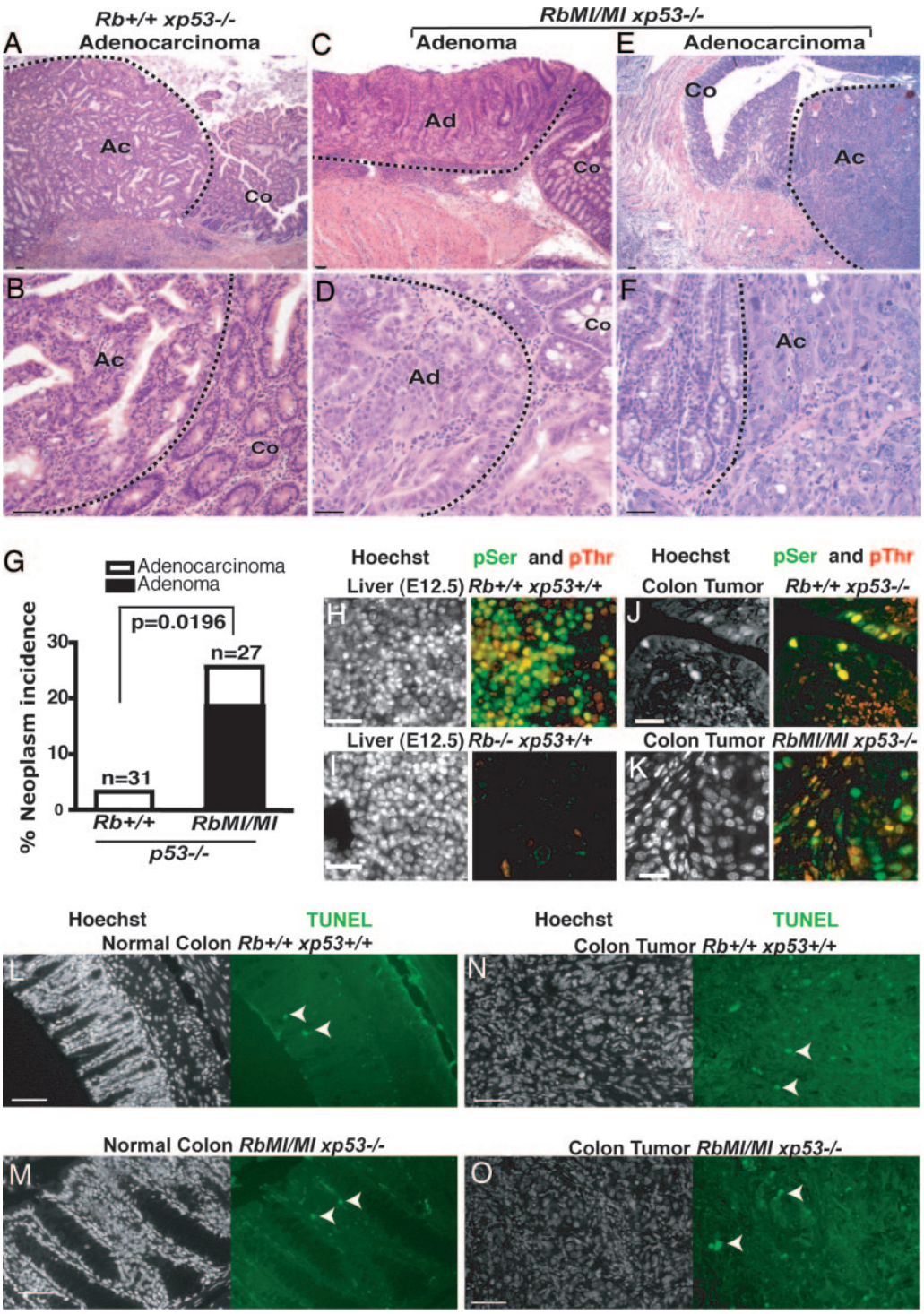

Fig. 2. Increased incidence of colon adenoma in the *Tm*($Rb^{MI/MI}xp53^{-/-}$) mice. (*A* and *B*) A rare adenocarcinoma of the *Tm*($Rb^{+/+}xp53^{-/-}$) genotype. (*C* and *D*) Representative adenomas from *Tm*($Rb^{MI/MI}xp53^{-/-}$) mice. (*E* and *F*) Adenocarcinoma of *Tm*($Rb^{MI/MI}xp53^{-/-}$) genotype. Dashed lines delineate tumors. *Ac*, adenocarcinoma; *Ad*, adenoma; *Co*, normal colon. (*G*) Histogram showing the incidence of adenomas and adenocarcinomas in the colons of mice with the indicated genotypes. The difference in colon tumor incidence is significant ($P = 0.0196$, Fisher's exact test). (*H–K*) The Rb-MI protein is phosphorylated in colon tumors. Photomicrographs of sections stained with bisbenzimide (Hoechst, left images) or anti-phosphoSer807/811 (green) and anti-phosphoThr821/826 (red) (right images). (*L–O*) Photomicrographs of sections stained with bisbenzimide (Hoechst, left images) or processed for TUNEL assay (green) (right images). Arrowheads indicate TUNEL-positive nuclei. Tissue types and genotypes are indicated above each photomicrograph. (Scale bars: 50 μm for *A–F* and *L–O*; 30 μm for *H–K*.)

phorylated Thr-821/826, to examine Rb and Rb-MI phosphorylation in tumors. These antibodies react with the mouse Rb protein because they stained nuclei in liver sections prepared from $Rb^{+/+}$ (Fig. 2*H*) but not from $Rb^{-/-}$ embryos (Fig. 2*I*). When tissue sections were pretreated with calf intestine alkaline phosphatase, staining by these phosphorylation-specific antibodies was reduced to background level (Fig. 5*A*, which is published as supporting information on the PNAS web site). These results

confirmed the specificity of these phospho-RB antibodies. Phosphorylated Rb or Rb-MI was detected in lymphomas, teratomas (Fig. 5 *B* and *C*) and colon tumors (Fig. 2 *J* and *K*). We noted a considerable heterogeneity in the relative phosphorylation signals among different cell types in normal and tumor tissues, indicating Rb and Rb-MI phosphorylation *in vivo* maybe complex and not simply determined by the cell cycle status (Figs. 2 *H*, *J*, and *K* and 5). Nevertheless, these results confirmed the expression and phosphorylation of Rb and Rb-MI proteins in tumors that developed in the *p53-null* mice.

In the colonic tumors, we could detect β-catenin and found its staining pattern to be similar among the $Tm(Rb^{MI/MI}xp53^{-/-})$ and $Tm(Rb^{+/+}xp53^{-/-})$ tumors (Fig. 6, which is published as supporting information on the PNAS web site). We observed membrane-associated β-catenin staining and cytoplasmic and nuclear staining (Fig. 6), indicating the β-catenin pathway is activated in these colonic tumors. The proliferation index as measured by staining for Ki-67 or proliferation nuclear antigen (proliferating cell nuclear antigen) was similar between tumors of $Tm(Rb^{+/+}xp53^{-/-})$ and $Tm(Rb^{MI/MI}xp53^{-/-})$ genotypes (Fig. 6). In normal colonic tissues, proliferating cell nuclear antigen-positive cells were restricted to the crypts and showed similar incidence among $Tm(Rb^{+/+}xp53^{-/-})$ and $Tm(Rb^{MI/MI}xp53^{-/-})$ mice (Fig. 6). The incidence of TUNEL-positive cells was very low, and the incidence was similar among the $Tm(Rb^{+/+}xp53^{-/-})$ and $Tm(Rb^{MI/MI}xp53^{-/-})$ mice, both in a normal colon (Fig. 2 *L* and *M*) and colon tumors (Fig. 2 *N* and *O*). Carcinomas from $Tm(Rb^{+/+}xp53^{-/-})$ and $Tm(Rb^{MI/MI}xp53^{-/-})$ mice showed an average of 22 and 21 TUNEL-positive cells per field (×400), respectively (Fig. 2 *N* and O). In normal epithelium, we found an average of 0.77 and 0.87 TUNEL-positive cells per crypt in $Tm(Rb^{+/+}xp53^{-/-})$ and $Tm(Rb^{MI/MI}xp53^{-/-})$ mice, respectively (Fig. 2 *L* and *M*). These results suggest that *Rb-MI* does not affect the steady-state levels of cell proliferation or apoptosis in normal or tumor tissues.

Reduced Apoptosis and Ulceration upon Colonic Injury in *Rb-MI* Mice. We have previously shown that fibroblasts of $Tm(Rb^{MI/MI}xp53^{-/-})$ genotype are resistant to TNF-induced apoptosis, but they remain sensitive to DNA damage-induced apoptosis (28). We compared the cell death response of $Tm(Rb^{+/+}xp53^{-/-})$ and $Tm(Rb^{MI/MI}xp53^{-/-})$ fibroblasts to several DNA damaging agents, including cisplatin, doxorubicin, etoposide, and camptothecin but could not detect any difference (data not shown). Thus, *Rb-MI* does not interfere with DNA damage-induced apoptosis either in p53-positive (28) or p53-negative cells (data not shown).

As previously described, *Rb-MI* mice exhibited reduced apoptosis in the intestine during endotoxic shock (21). To further determine whether *Rb-MI* affords protection of colonic epithelium without the complication of a systemic shock response, we adopted an *in vivo* model of colonic epithelial injury by exposing mice to DSS in the drinking water (34). We first examined the tissues for apoptotic cell death after 3 days of exposure to DSS. We found the level of TUNEL-positive nuclei in the epithelium from DSS-treated $Tm(Rb^{MI/MI}xp53^{-/-})$ mice to be significantly lower than that of $Tm(Rb^{+/+}xp53^{-/-})$ mice (Fig. 3*C*). We then exposed the mice to DSS for 7 days; this prolonged exposure is known to cause ulceration, resulting, in part, from the destruction of epithelial cells. Histological examination after 7 days of DSS treatment showed that the size of ulcers, which were restricted to the colorectal region, was significantly reduced in $Tm(Rb^{MI/MI}xp53^{-/-})$ mice in comparison with $Tm(Rb^{+/+}xp53^{-/-})$ mice (Fig. 3*G*). Despite the similar levels of consumption of DSS water, the average weight loss was greater with $Tm(Rb^{+/+}xp53^{-/-})$ mice (−14%) than with $Tm(Rb^{MI/MI}xp53^{-/-})$ mice (−9%) after 7 days. The protection of colonic epithelium from injury-induced destruction by

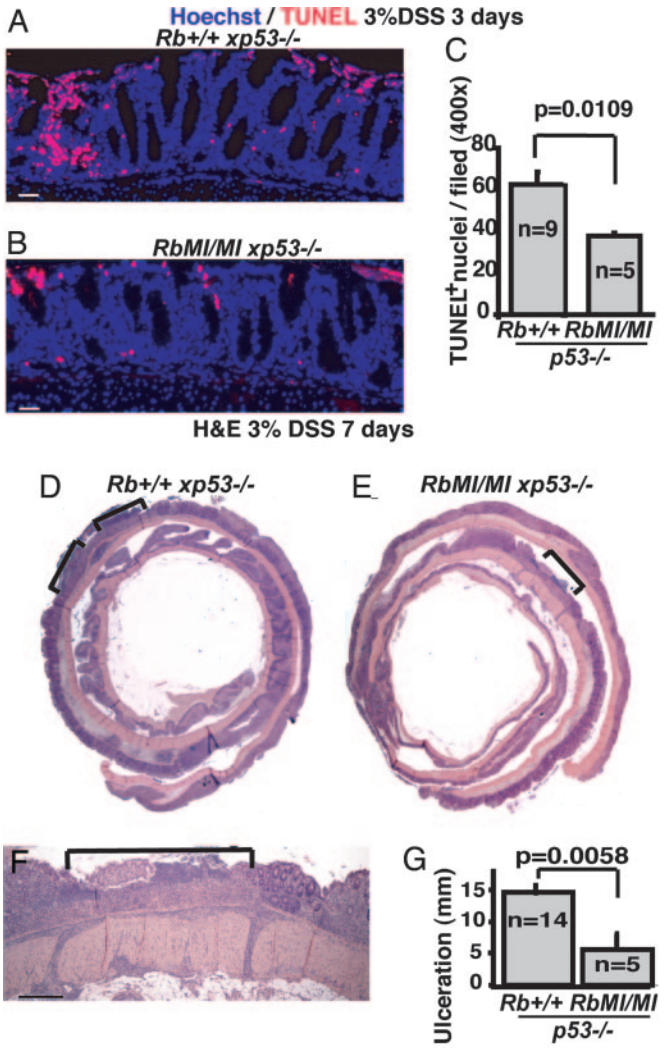

Fig. 3. *Rb-MI* attenuates colonic epithelial cell death and ulceration induced by DSS. (*A* and *B*) Representative photomicrographs of colon sections processed for TUNEL assay (red) and counterstained with bisbenzimide (Hoechst-blue) from $Tm(Rb^{+/+}xp53^{-/-})$ (*A*) and $Tm(Rb^{MI/MI}xp53^{-/-})$ mice (*B*) treated with 3% DSS for 3 days. (*C*) Histogram shows the number of TUNEL-positive nuclei with s.e.m. in the distal colon from animals treated with 3% DSS for 3 days with the indicated genotypes. (*D–F*) Representative photomicrographs of hematoxylin/eosin-stained paraffin sections of the entire colon (*D* and *E*) or higher magnification showing ulcers (*F*) after 7 days of DSS treatment. The area of ulcers is marked in the figures. The mucosa and submucosa were heavily infiltrated with inflammatory cells (*F*). (*G*) Histogram shows the mean plus s.e.m. of the total size of ulcers after 7 days of DSS treatment with the indicated genotypes. *P* values are indicated in each histogram (unpaired *t* test). (Scale bars: 60 μm in *A*, *B*, and *F*; 240 μm in *D* and *E*.)

Rb-MI is consistent with increased colonic tumor formation in *Rb-MI/p53-null* mice.

Discussion

Results from this study support the conclusion that caspase-resistant *Rb-MI* can promote tumor development. Tumor promotion by *Rb-MI* can be observed in the *p53-null* genetic background and displays tissue specificity that is consistent with its anti-apoptotic effect. The *Rb-MI* allele does not affect the development of lymphomas, the most prevalent tumor type in *p53-null* mice (Fig. 4). This result is in keeping with previous observations that *Rb-MI* does not reduce thymic or splenic apoptosis induced by ionizing radiation or endotoxin, respec-

tively (28). Instead, *Rb-MI* increases the incidence of colonic adenomas (Fig. 2), consistent with reduced intestinal apoptosis previously observed with *Rb-MI* mice during endotoxic shock (28). The *Rb-MI* allele also exacerbated the teratoma phenotype associated with p53-knockout in the 129-mouse genetic background (ref. 31 and Fig. 1). A previous study has demonstrated that p53 and FAS are both involved in germ cell apoptosis after heat stress (35). Whether *Rb-MI* can reduce germ cell apoptosis remains to be determined.

The Rb-MI protein is expressed and phosphorylated in the colonic tumors (Fig. 2). Phosphorylation of Rb disrupts its interaction with E2F, Abl, and LxCxE-containing proteins (36–38), resulting in increased proliferation and sensitization to apoptosis (3). This Rb phosphorylation-associated sensitivity to apoptosis would be blunted by the *p53-null* background, which is known to protect *Rb*-deficient cells from undergoing apoptosis (3, 18, 19). We have previously shown that Rb-MI prevents TNF from activating the nuclear Abl tyrosine kinase; the inhibition of Abl contributes in part to protection from TNF-induced cell death (12). We have also shown that Ser-807/811 phosphorylation disrupts RB–Abl interaction (38). Thus, Ser-807/811-phosphorylated Rb-MI is not likely to prevent apoptosis through the inhibition of Abl. Because phosphorylated Rb-MI is detected in colonic tumor tissues, it is possible that Rb-MI can provide additional apoptotic protection, which is not disrupted by phosphorylation. Whether a phosphorylation-resistant anti-apoptotic function of Rb-MI contributed to colonic tumor formation remains to be determined.

The caspase-resistant Rb-MI does not protect against apoptosis induced by ionizing radiation or doxorubicin (28). We have found that *Rb-MI* exerts no protection to several other genotoxins, i.e., etoposide, cisplatin, camptothecin, and menadione, even in the *p53-null* genetic background. Our results suggest that *Rb-MI* does not affect the steady-state levels of proliferation or apoptosis in colonic tissues. However, *Rb-MI* can protect the colonic epithelium from apoptosis that is associated with injuries caused by DSS, resulting in reduced ulcers (Fig. 3). We found that $p53^{-/-}$ mice were more sensitive than $p53^{+/+}$ mice to DSS exposure, exhibiting more weight loss and larger ulcers (data not shown). This observation is consistent with a recent report that *p53-null* mice are prone to inflammation due, in part, to enhanced NF-κB activity (39). We have previously found that *Rb-MI* does not affect the apoptotic response of splenocytes or macrophages to endotoxin (28) (I. Hunton and J.Y.J.W., unpublished data), indicating the unlikelihood of *Rb-MI* to promote inflammation. Taken together, these observations suggest that the colonic tumor development in $Tm(Rb^{MI/MI}xp53^{-/-})$ mice may be associated with increased inflammation due to the loss of p53 and decreased apoptotic response due to the expression of caspase-resistant Rb-MI.

It is interesting to note that *RB* gene mutations have been detected in a wide variety of sporadic human cancers except those of the large intestine (Sanger Institute Genome Database, www.sanger.ac.uk). Instead, the RB protein level is elevated in some colorectal tumors, and the knockdown of RB causes death of these tumor cells (40) (N.B. Chau and J.Y.J.W., unpublished observations). The nucleotide sequencing of *RB* in sporadic human cancers has focused on exons that encode the RB A/B pockets, which are important for its tumor suppression function. The C-terminal caspase cleavage site is encoded by *RB*-exon 25, which is dispensable for the *RB* tumor suppression function and, hence, has not been sequenced in human cancers. In addition to *RB*-exon 25 mutations, the loss of caspase or the gain of caspase inhibitors can also disrupt the cleavage of RB; results from this study suggest that these events may contribute to colonic tumor development.

We thank Dr. Jonathan J. Zhu for assistance in statistical analyses and Irina C. Hunton, Guizhen Sun, and Rimma Levenzon for providing critical technical support. L.E. is supported by National Institutes of Health Grant RR17030. This study was funded by National Institutes of Health Grant CA58320 (to J.Y.J.W.).

1. Hanahan, D. & Weinberg, R. A. (2000) *Cell* **100,** 57–70.
2. Sherr, C. J. & McCormick, F. (2002) *Cancer Cell* **2,** 103–112.
3. Chau, B. N. & Wang, J. Y. (2003) *Nat. Rev. Cancer* **3,** 130–138.
4. Liu, H., Dibling, B., Spike, B., Dirlam, A. & Macleod, K. (2004) *Curr. Opin. Genet. Dev.* **14,** 55–64.
5. Mittnacht, S. (2005) *Eur. J. Cell Biol.* **84,** 97–107.
6. Moroni, M. C., Hickman, E. S., Denchi, E. L., Caprara, G., Colli, E., Cecconi, F., Muller, H. & Helin, K. (2001) *Nat. Cell Biol.* **3,** 552–558.
7. Nahle, Z., Polakoff, J., Davuluri, R. V., McCurrach, M. E., Jacobson, M. D., Narita, M., Zhang, M. Q., Lazebnik, Y., Bar-Sagi, D. & Lowe, S. W. (2002) *Nat. Cell Biol.* **4,** 859–864.
8. Leone, G., Sears, R., Huang, E., Rempel, R., Nuckolls, F., Park, C. H., Giangrande, P., Wu, L., Saavedra, H. I., Field, S. J., *et al.* (2001) *Mol. Cell* **8,** 105–113.
9. Hallstrom, T. C. & Nevins, J. R. (2003) *Proc. Natl. Acad. Sci. USA* **100,** 10848–10853.
10. Wang, J. Y. (2000) *Oncogene* **19,** 5643–5650.
11. Wang, J. Y. (2005) *Cell Res.* **15,** 43–48.
12. Chau, B. N., Chen, T. T., Wan, Y. Y., DeGregori, J. & Wang, J. Y. (2004) *Mol. Cell. Biol.* **24,** 4438–4447.
13. Irwin, M., Marin, M. C., Phillips, A. C., Seelan, R. S., Smith, D. I., Liu, W., Flores, E. R., Tsai, K. Y., Jacks, T., Vousden, K. H. & Kaelin, W. G., Jr. (2000) *Nature* **407,** 645–648.
14. Attwooll, C., Denchi, E. L. & Helin, K. (2004) *EMBO J.* **23,** 4709–4716.
15. Bracken, A. P., Ciro, M., Cocito, A. & Helin, K. (2004) *Trends Biochem. Sci.* **29,** 409–417.
16. Sears, R. C. & Nevins, J. R. (2002) *J. Biol. Chem.* **277,** 11617–11620.
17. Lissy, N. A., Davis, P. K., Irwin, M., Kaelin, W. G. & Dowdy, S. F. (2000) *Nature* **407,** 642–645.
18. Bates, S., Phillips, A. C., Clark, P. A., Stott, F., Peters, G., Ludwig, R. L. & Vousden, K. H. (1998) *Nature* **395,** 124–125.
19. Kamijo, T., Weber, J. D., Zambetti, G., Zindy, F., Roussel, M. F. & Sherr, C. J. (1998) *Proc. Natl. Acad. Sci. USA* **95,** 8292–8297.
20. Vella, V., Zhu, J., Frasca, F., Li, C. Y., Vigneri, P., Vigneri, R. & Wang, J. Y. (2003) *J. Biol. Chem.* **278,** 25151–25157.
21. Lin, B. T., Gruenwald, S., Morla, A. O., Lee, W. H. & Wang, J. Y. (1991) *EMBO J.* **10,** 857–864.
22. Lees, J. A., Buchkovich, K. J., Marshak, D. R., Anderson, C. W. & Harlow, E. (1991) *EMBO J.* **10,** 4279–4290.
23. Hinds, P. W., Mittnacht, S., Dulic, V., Arnold, A., Reed, S. I. & Weinberg, R. A. (1992) *Cell* **70,** 993–1006.
24. Knudsen, E. S., Buckmaster, C., Chen, T. T., Feramisco, J. R. & Wang, J. Y. (1998) *Genes Dev.* **12,** 2278–2292.
25. Tan, X. & Wang, J. Y. (1998) *Trends Cell Biol.* **8,** 116–120.
26. Tan, X., Martin, S. J., Green, D. R. & Wang, J. Y. (1997) *J. Biol. Chem.* **272,** 9613–9616.
27. Boutillier, A. L., Trinh, E. & Loeffler, J. P. (2000) *Oncogene* **19,** 2171–2178.
28. Chau, B. N., Borges, H. L., Chen, T. T., Masselli, A., Hunton, I. C. & Wang, J. Y. (2002) *Nat. Cell Biol.* **4,** 757–765.
29. Jacks, T., Remington, L., Williams, B. O., Schmitt, E. M., Halachmi, S., Bronson, R. T. & Weinberg, R. A. (1994) *Curr. Biol.* **4,** 1–7.
30. Welch, P. J. & Wang, J. Y. (1993) *Cell* **75,** 779–790.
31. Donehower, L. A., Harvey, M., Vogel, H., McArthur, M. J., Montgomery, C. A., Jr., Park, S. H., Thompson, T., Ford, R. J. & Bradley, A. (1995) *Mol. Carcinog.* **14,** 16–22.
32. Boivin, G. P., Washington, K., Yang, K., Ward, J. M., Pretlow, T. P., Russell, R., Besselsen, D. G., Godfrey, V. L., Doetschman, T., Dove, W. F., *et al.* (2003) *Gastroenterology* **124,** 762–777.
33. Solnick, J. V. & Schauer, D. B. (2001) *Clin. Microbiol. Rev.* **14,** 59–97.
34. Greten, F. R., Eckmann, L., Greten, T. F., Park, J. M., Li, Z. W., Egan, L. J., Kagnoff, M. F. & Karin, M. (2004) *Cell* **118,** 285–296.
35. Yin, Y., Stahl, B. C., DeWolf, W. C. & Morgentaler, A. (2002) *J. Androl.* **23,** 64–70.
36. Knudsen, E. S. & Wang, J. Y. (1998) *Oncogene* **16,** 1655–1663.
37. Knudsen, E. S. & Wang, J. Y. (1997) *Mol. Cell. Biol.* **17,** 5771–5783.
38. Knudsen, E. S. & Wang, J. Y. (1996) *J. Biol. Chem.* **271,** 8313–8320.
39. Komarova, E. A., Krivokrysenko, V., Wang, K., Neznanov, N., Chernov, M. V., Komarov, P. G., Brennan, M. L., Golovkina, T. V., Rokhlin, O., Kuprash, D. V., *et al.* (2005) *FASEB J.* **19,** 1030–1032.
40. Yamamoto, H., Soh, J. W., Monden, T., Klein, M. G., Zhang, L. M., Shirin, H., Arber, N., Tomita, N., Schieren, I., Stein, C. A. & Weinstein, I. B. (1999) *Clin. Cancer Res.* **5,** 1805–1815.